The synthesis and structural mapping of unsymmetrical chemically modified α-cyclodextrins by high-field nuclear magnetic resonance spectroscopy

Peter R. Ashton, Edward Y. Hartwell, Douglas Philp, Neil Spencer * and J. Fraser Stoddart
School of Chemistry, University of Birmingham, Edgbaston, Birmingham, UK B15 2TT

Hexakis(2,3-di-*O*-methyl-6-deoxy-6-iodo)-α-cyclodextrin (I-DMαCD) was prepared from hexakis(2,3-di-*O*-methyl)-αCD (DMαCD) using iodine and triphenylphosphine. The subsequent attempted substitution of I-DMαCD with the phenoxide anions of either 4-hydroxybenzyl alcohol or 4-benzyloxyphenol produced unexpected products. These products were found to be a result of an elimination reaction involving one of the iodomethyl groups to produce one 6-deoxyhex-5-eno-D-glucopyranoside residue within the DMαCD structure in addition to the substitution of the other five iodomethyl groups either by (4-hydroxymethyl)-phenyl or by (4-benzyloxy)phenyl ether functions, respectively. The products have been characterised fully using high resolution positive-ion FABMS and high resolution ^1H and ^{13}C NMR spectroscopies.

The wide-ranging ability of cyclodextrins (CDs) to form inclusion complexes with a large variety of guest species is now well documented[1] and the complexes which result have many potential, as well as demonstrated, applications.[2] One such application—the ability to use a CD complex in order to carry out a regioselective modification of the guest species—has also been studied, most notably by Breslow[3] and Komiyama.[4] It is this aspect of their use that aroused our interest in chemically modified CDs. Recently, we have been attempting to modify CDs by the formation of phenyl ether moieties on the primary face of the CD in an attempt to produce a deeper, more rigid cavity to allow the enhanced complexation of phenols. The outcome of this research programme has resulted in the synthesis of some new chemically modified CDs, which are themselves suitable substrates for further elaboration. With one particular CD, namely hexakis(2,3-di-*O*-methyl-6-deoxy-6-iodo)-α-CD, we encountered problems in fully substituting the molecule with phenoxide nucleophiles and obtained some unexpected products. Although there is a large amount of literature[5] available regarding unsymmetrical CDs, very few reports provide a full NMR spectroscopic characterisation for these compounds. Also, very few papers report full mass spectroscopic characterisation evidence for unsymmetrical CDs. Here, we present the synthesis of two new, unusual, highly modified CDs containing single 6-deoxyhex-5-eno-D-glucopyranoside units and their characterisation and investigation to a high level of understanding by FABMS and NMR spectroscopy.

Results and discussion

As part of our investigations into the regioselective chlorination of disubstituted benzene derivatives using CDs as supramolecular reaction vessels, we prepared hexakis(2,3-di-*O*-methyl)-α-CD (DMαCD)[6] in an effort to direct the chlorination of monosubstituted phenols towards the exposed *para* position. Unfortunately, following the investigation of its directing properties, further modification of DMαCD was found to be necessary. In our attempts to modify DMαCD, a new modified CD, hexakis(2,3-di-*O*-methyl-6-deoxy-6-iodo)-α-CD (I-DMαCD) was synthesised from DMαCD to allow the straightforward coupling of phenols to the primary C-6 positions of DMαCD. Difficulties were encountered, however, when attempting the complete substitution of I-DMαCD with 4-hydroxybenzyl alcohol (4-HBA) in acetonitrile using anhydrous potassium carbonate as base. Analysis of the reaction mixture using positive-ion fast atom bombardment mass spectrometry (FABMS) revealed two major products. Preparative reversed-phase HPLC separation of the mixture afforded the fully substituted product hexakis[2,3-di-*O*-methyl-6-*O*-(4-hydroxymethylphenyl)]-α-cyclodextrin (4-HMP-DMαCD) in 7% yield and a second product in 20% yield. Low resolution positive-ion FABMS recorded on 4-HMP-DMαCD showed a signal at *m/z* 1799 for $[M + Na]^+$ whereas the second product afforded a signal at *m/z* 1675 for $[M + Na]^+$. The molecular weight observed for the second product was consistent with two possible structures, differing by two mass units—both containing five (4-hydroxymethyl)phenyl residues. However, an unequivocal structural assignment could not be carried out on the basis of the mass spectroscopic evidence alone. The FABMS data raised a question about the nature of the substituent at the C-6 position on one of the glucopyranose residues within the molecule. The two possibilities were for reduction to have occurred at the C-6 position in question, to yield a methyl group, or for elimination to have taken place to produce one 6-deoxyhex-5-eno-D-glucopyranoside residue within the α-CD molecule affording 6^A-deoxy-5^A,6^A-didehydro-2^A,2^B,2^C,2^D,2^E,2^F,3^A,3^B,3^C,3^D,3^E,3^F-dodeca-*O*-methyl-6^B,6^C,6^D,6^E,6^F-penta-*O*-(4-hydroxymethylphenyl)-α-cyclodextrin, $(4\text{-HMP})_5$-eno-DMαCD. Although reported recently in disaccharide chemistry,[7] the elimination reaction is unknown in the field of CD research. A full NMR spectroscopic assignment was thus undertaken to determine the precise structure of the molecule with respect to the pyranosidic residues and indeed, the product turned out to be the elimination product $(4\text{-HMP})_5$-eno-DMαCD, which was confirmed by high resolution FABMS. In the course of this investigation, a further example of the elimination reaction was observed. Treatment of I-DMαCD with 4-benzyloxyphenol (4-BOP) resulted in the isolation of 5^A,6^A-deoxy-5^A,6^A-didehydro-2^A,2^B,2^C,2^D,2^E,2^F,3^A,3^B,3^C,3^D,3^E,3^F-dodeca-*O*-methyl-6^B,6^C,6^D,6^E,6^F-penta-*O*-(4-benzyloxyphenyl)-α-cyclodextrin, $(4\text{-BOP})_5$-eno-DMαCD, in 6% yield. The full ^1H NMR spectroscopic assignment of this latter compound is also presented.

Having confirmed that the new unsymmetrical structures contained one 6-deoxyhex-5-eno-D-glucopyranoside unit, we are able to reach some conclusions about the nature of the

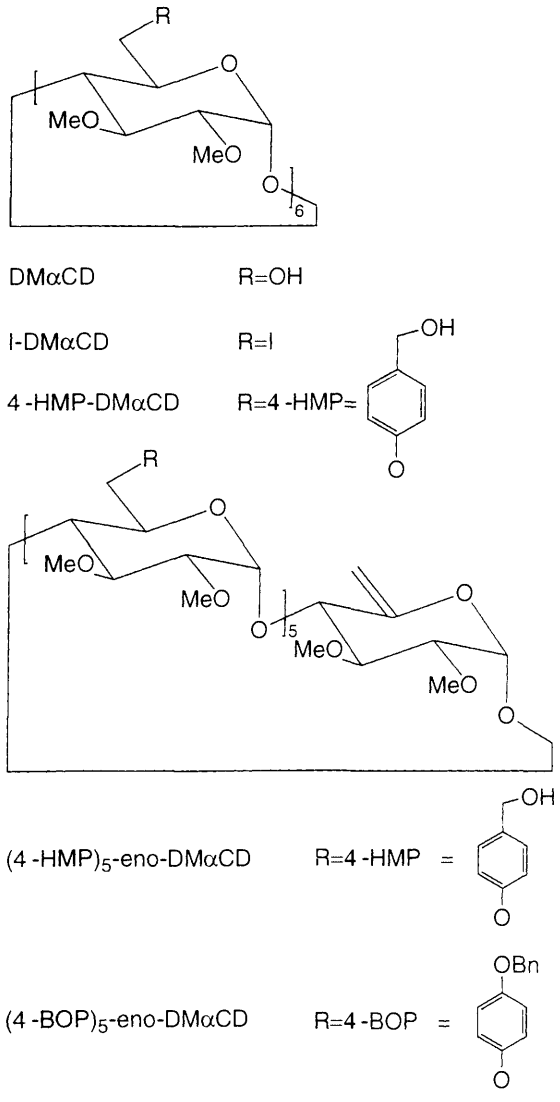

chemistry leading to these products. The first difficulty lay in accepting that potassium carbonate, acting as a base, was capable of performing an elimination reaction at the iodomethyl groups. In an attempt to shed some light on the situation, a control reaction was carried out in which I-DMαCD was dissolved in dry acetonitrile and stirred with anhydrous potassium carbonate for one week. Analysis of the reaction mixture by reversed-phase HPLC and positive ion FABMS revealed that only starting material was present. We are therefore confident that the elimination is not promoted by potassium carbonate and it must therefore be promoted by the phenoxide ions in the reactions in question. However, this is a surprising result since, the pK_as of the two reagents are almost identical—the pK_a of a phenoxide ion is in the range 8–11 and the pK_a for a carbonate ion is 10.3. The difference in the reactivity can therefore be ascribed to the phenoxide ion being highly solvated in acetonitrile, the solvent for the reaction, and the carbonate being virtually insoluble.

From the yields obtained in the reaction between I-DMαCD and 4-HBA, it is clear that (4-HMP)$_5$-eno-DMαCD is formed in preference to the fully substituted compound, 4-HMP-DMαCD. The fact that elimination of HI only occurs at one D-glucopyranose unit in the CD does not mean that the elimination is not a competing process with all the other substitutions of the iodomethyl groups. We must assume that elimination can take place at all iodomethyl groups in the

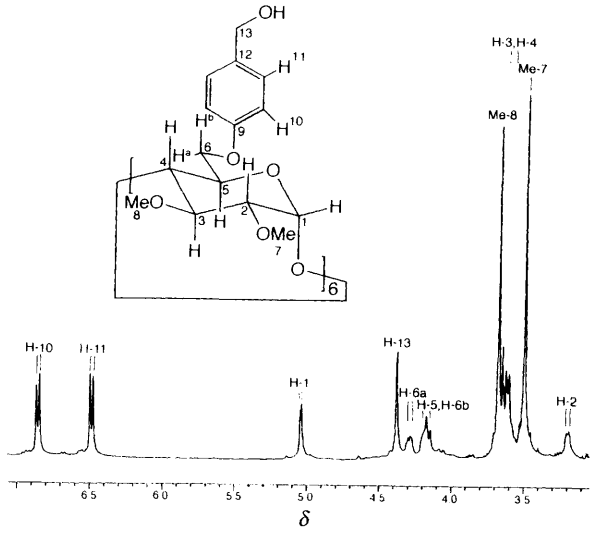

Fig. 1 The ^{1}H NMR spectrum for 4-HMP-DMαCD (400 MHz; $CDCl_3$; 22 °C; ref. Me_4Si)

CD molecule. For the most part, the nucleophilic substitution process occurs preferentially over elimination; however, mono-elimination must be a favoured process.

An explanation for the preference to form the mono-eliminated product may arise from the steric demands placed on the molecule when five 4-HMP groups are attached to the CD structure. In this situation, the nucleophile is hindered in its approach towards the iodomethyl group. Moreover, the 180° attack angle relationship preferred between the nucleophile and the leaving group, in the S_N2 reaction, is less easily satisfied and, as a result, the activation energy of the reaction is increased and the reaction becomes kinetically disfavoured. Further, elimination of HI is now a more favourable process as there are fewer constraints placed on the 'attack angle' in this reaction. Molecular models suggest this rationale to be valid as there is obviously severe steric congestion present in the region of the iodomethyl group. In the second reaction, namely that between I-DMαCD and 4-benzyloxyphenol, only a trace of the fully substituted product is observed in the positive-ion FABMS of the reaction mixture and this product was never isolated. It can therefore be assumed that the steric bulk around the final iodo group is too overwhelming to allow the approaching nucleophile to adopt a 180° relationship with the leaving group for a nucleophilic substitution reaction and instead, it reacts solely as a base, promoting the elimination of HI and the formation of (4-BOP)$_5$-eno-DMαCD.

The fully substituted compound 4-HMP-DMαCD, features six constitutionally equivalent pyranosidic residues resulting in a compound with C_6 symmetry and accordingly, the observed ^{1}H and ^{13}C spectra are effectively those of a single gluco-pyranose residue. The ^{1}H NMR spectrum of the fully symmetrical compound 4-HMP-DMαCD is shown in Fig. 1. The assignments were made on the basis of 2D-COSY and 2D-ROESY spectra and are consistent with those of other literature-reported, chemically modified cyclodextrins.[8] The chemical shift data for 4-HMP-DMαCD are listed in Table 1 and the coupling constant data in Table 2. The ^{13}C assignment data for the symmetrical compound 4-HMP-DMαCD were made on the basis of a 2D-CH correlation experiment and the assignments are given in Table 3.

For (4-HMP)$_5$-eno-DMαCD, where the elimination reaction has taken place, much more complex ^{1}H and ^{13}C NMR spectra are observed. The symmetry of the CD torus has been completely destroyed and each pyranosidic residue becomes

Table 1 ^{1}H NMR chemical shifts (ppm) for (4-HMP)$_5$-eno-DMαCD and 4-HMP-DMαCD (400 MHz; $CDCl_3$; 22 °C)

	(4-HMP)$_5$-eno-DMαCD[a]						
Proton	A (Red)	B (Orange)	C (Purple)	D (Blue)	E (Yellow)	F (Green)	4-HMP-DMαCD
H-1	5.03	4.97	5.05	5.01	5.07	5.14	5.05
H-2	3.32	3.13	3.16	3.16	3.23	3.23	3.20
H-3	3.68	3.59	3.62	3.66	3.63	3.73	3.66
H-4	3.99	3.67	3.62	3.59	3.63	3.73	3.66
H-5	N/A	4.09	4.02	4.10	4.17	4.39	4.18
H-6[a]	4.64	4.11	4.08	4.01	4.13	4.39	4.18
H-6[b]	5.13	4.31	4.19	4.27	4.31	4.39	4.32
H-7	3.52	3.44	3.49	3.48	3.50	3.51	
H-8	3.63			3.64, 3.66, 3.68, 3.69, 3.71			
H-13							4.45

[a] The residues are labelled according to Fig. 3. [b] H6a and H6b can be identified from coupling considerations.[34,35]

Table 2 Coupling constants[a] (Hz) for (4-HMP)$_5$-eno-DMαCD and 4-HMP-DMαCD

	(4-HMP)$_5$-eno-DMαCD[b]						
$^3J_{H,H}$	A	B	C	D	E	F	4-HMP-DMαCD
$^3J_{1,2}$	4.0	5.0	4.0	5.0	4.0	4.0	4.0
$^3J_{2,3}$	7.0	10.0	10.0	10.0	9.0	9.0	9.5
$^3J_{3,4}$	9.0	8.0	9.0	8.0	8.0	9.0	
$^3J_{4,5}$	N/A	10.0	11.0	10.0	11.0	11.0	
$^3J_{5,6a}$	N/A			Not accessible			4.5[c]
$^3J_{5,6b}$	N/A	4.0	5.0	5.0	4.0	4.0	
$^3J_{6a,6b}$	Broad	11.0	10.0	11.0	11.0	Not accessible	10.5

[a] The data are taken from the DQFCOSY spectrum (400 MHz; $CDCl_3$; 22 °C). The overlap of signals prevented the unravelling of coupling constants not quoted. The coupling constants were measured and rounded to the nearest integer to respect the digitisation limits of the experiment. [b] The residues are labelled according to Fig. 3. [c] See refs. 34 and 35.

Table 3 ^{13}C NMR chemical shifts (ppm) for (4-HMP)$_5$-eno-DMαCD and 4-HMP-DMαCD (100.6 MHz; $CDCl_3$; 22 °C)

	(4-HMP)$_5$-eno-DMαCD[a]						
Carbon	A	B	C	D	E	F	4-HMP-DMαCD
C-1	100.3	99.0	100.0	99.9	99.3	99.7	100.1
C-2	80.8	81.5	81.5	82.0	81.9	81.9	82.0
C-3	80.5	81.6	82.4	81.9	81.7	81.8	82.9
C-4	81.1	81.6	82.7	82.4	81.7	82.2	81.6
C-5	154.3	70.6	71.1	70.9	71.0	71.4	71.0
C-6	98.9			68.0, 67.7[b]		67.5	67.9
C-7	58.1	57.8	58.3	58.0	57.9	58.6	58.1
C-8	60.9			61.8, 61.7, 61.6			61.9
C-9				158.1, 158.0, 157.9, 157.8			157.9
C-10				115.3, 114.8, 114.6, 114.5			114.8
C-11				129.6, 128.5, 128.4, 128.3, 120.4			128.4
C-12				133.6, 133.5, 133.3			133.5
C-13				64.4, 64.3, 64.2, 64.2			64.5

[a] The residues are labelled according to Fig. 3. [b] The C6/H6 correlation in the 2D experiment was not observed: see the text.

magnetically inequivalent, each having its own set of resonances. The more complex ^{1}H NMR spectrum of the unsymmetrical compound (4-HMP)$_5$-eno-DMαCD is shown in Fig. 2(*a*)–(*e*). The justification for these assignments is discussed below. We have not assigned any of the aromatic protons for the 4-HMP group at position 6 to specific pyranosidic residues.

The compound descriptors that we have adopted in this paper are based on a nomenclature system for CDs introduced by Tabushi *et al.*[9] The pyranosidic unit containing the olefinic double bond in (4-HMP)$_5$-eno-DMαCD and (4-BOP)$_5$-eno-DMαCD has been designated as residue A. The remaining five constitutionally heterotopic pyranosidic units have been labelled B, C, D, E and F in a clockwise direction [Fig. 3(*a*)] when the CD torus is viewed from the face originally bearing the secondary hydroxy groups, *i.e.*, viewed in a clockwise direction following the glycosidic bond from C1→C4. The numbering system we have used for the nuclei in the NMR spectroscopic assignments is also shown in Fig. 3(*b*). In this paper, we have chosen to use colour for clarity in the figures showing the spin systems for each pyranosidic unit. For residue A, the constitutionally different pyranosidic unit which features the exocyclic double bond, the spin system is readily identified and has been coloured red in the figures. The spin systems of the other five rings, which we have coloured orange, purple, blue, yellow and green in the figures do, in fact, have the connectivity pattern that we have designated in Fig. 3, as will be shown in the discussion section. In order to avoid confusion, this labelling system will be adopted from the outset.

Each of the six pyranosidic spin systems was identified by performing a 2D-HOHAHA experiment. From a comparison of the ^{1}H NMR spectrum of the symmetrical compound 4-HMP-

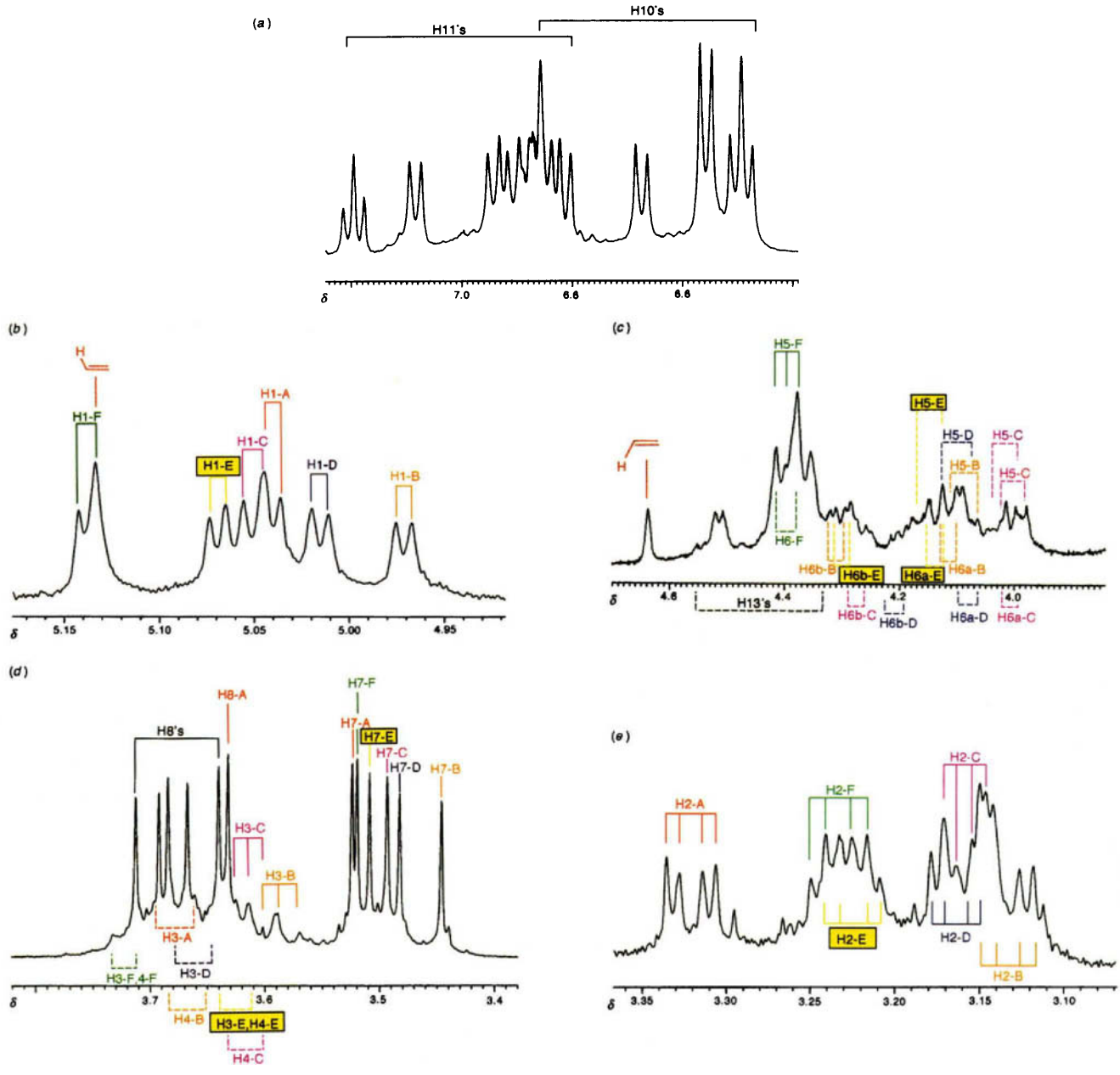

Fig. 2 The ^{1}H NMR spectrum of (4-HMP)$_5$-eno-DMαCD (400 MHz; $CDCl_3$; 22 °C; ref. Me_4Si) presented as a sequence (*a*), (*b*), (*c*), (*d*), (*e*) of partial spectra. The assigned signals are numbered according to the usual convention shown in Fig. 3(*b*): the capital letters refer to the residue sequence defined in Fig. 3(*a*).

DMαCD shown in Fig. 1, the resonances between δ 4.9 and δ 5.2 are readily assigned to be those of the protons on the anomeric C1 centres—a separate doublet is clearly evident for each of the six heterotopic anomeric protons. Fig. 4(*a*) shows the partial 2D-HOHAHA spectrum in which the cross peaks for the six rows of anomeric protons are clearly displayed. A point of interest is that the six spin systems are totally discrete, *i.e.*, there is no coupling observed for an anomeric proton to the H4 proton of the neighbouring pyranosidic unit across the glycosidic linkage. An examination of the data displayed in Fig. 4(*a*) at a slightly deeper contour level allows the five sets of H6 protons in residues B to F to be assigned. This spectrum is shown in Fig. 4(*b*).

Fig. 4(*a*) also clearly shows one of the cross peaks (at δ 4.64) for the exocyclic olefinic protons on ring A and the correlation of this proton into the anomeric proton and H4 of the same ring. [The AX system for these olefinic protons is clearly visible in the partial 1D, ^{1}H spectrum in Figs. 2(*b*) and 2(*c*) at δ 5.13 and δ 4.64.]

The respective H2 and H3 assignments were made simply by performing a 2D double quantum filtered (DQF)-COSY experiment. The correlation between H3 and H4 for ring A (coloured red in the figures) is also unequivocal since this particular ring does not possess an H5 proton—this proton has been eliminated in the formation of the exocyclic double bond. The DQF-COSY experiment also confirms the assignments shown in Fig. 4(*b*) for the H6 protons.

To prove unequivocally the H5/H4 assignments for the remaining pyranosidic rings, the DQF-COSY data in the H6 area was further examined. A partial projection of this spectral area is shown in Fig. 5. With the exception of the H5 protons for ring F (coloured green in the figures), the remaining four H5 protons are clearly visible at chemical shift positions described by the 2D-HOHAHA experiment. In turn, the cross peaks in the 2D-DQF-COSY experiment locate the positions of their respective H6 protons. Having located all the H5 protons, the H4 protons are the remaining unassigned signals in the HOHAHA spectrum. The DQF-COSY spectrum is

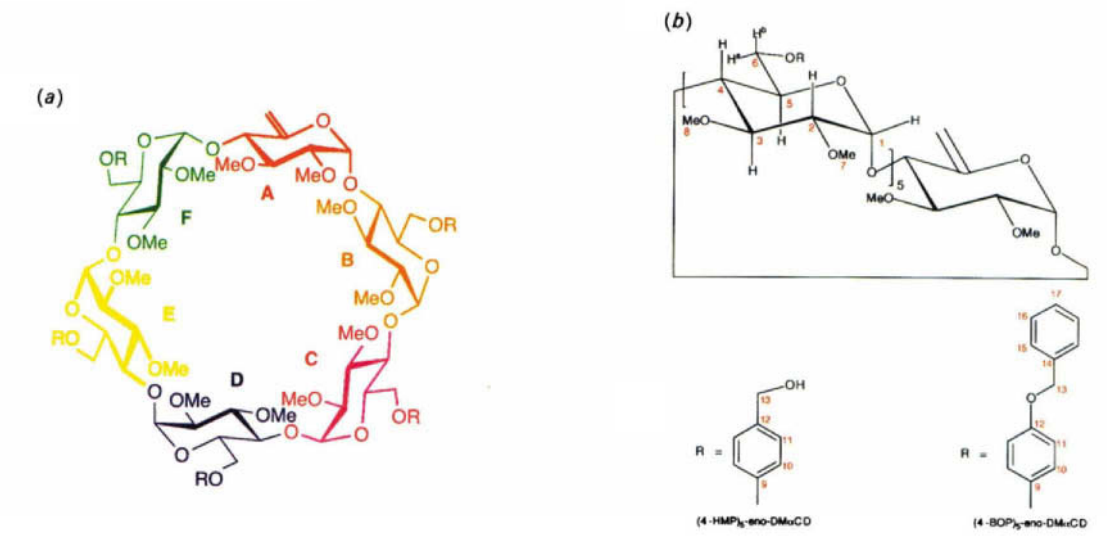

Fig. 3 (*a*) The full general structural formula of a DMαCD derivative containing one 6-deoxy-5-enopyranoside residue. The ring-labelling sequence (A–F) is given. (*b*) The structural formula for one 6-*O*-substituted-2,3-di-*O*-methyl-D-glucopyranose residue 4-HMP-eno-DMαCD and 4-BOP-eno-DMD showing the notation used, particularly for H-6. Only the *gauche–gauche* conformation of the C(5)–C(6) bond is depicted. The H6a/H6b notation adopted is that according to Saenger [34] and Sadler,[35] where H6b is designated as that proton showing the largest coupling of the two H6 protons with H5.

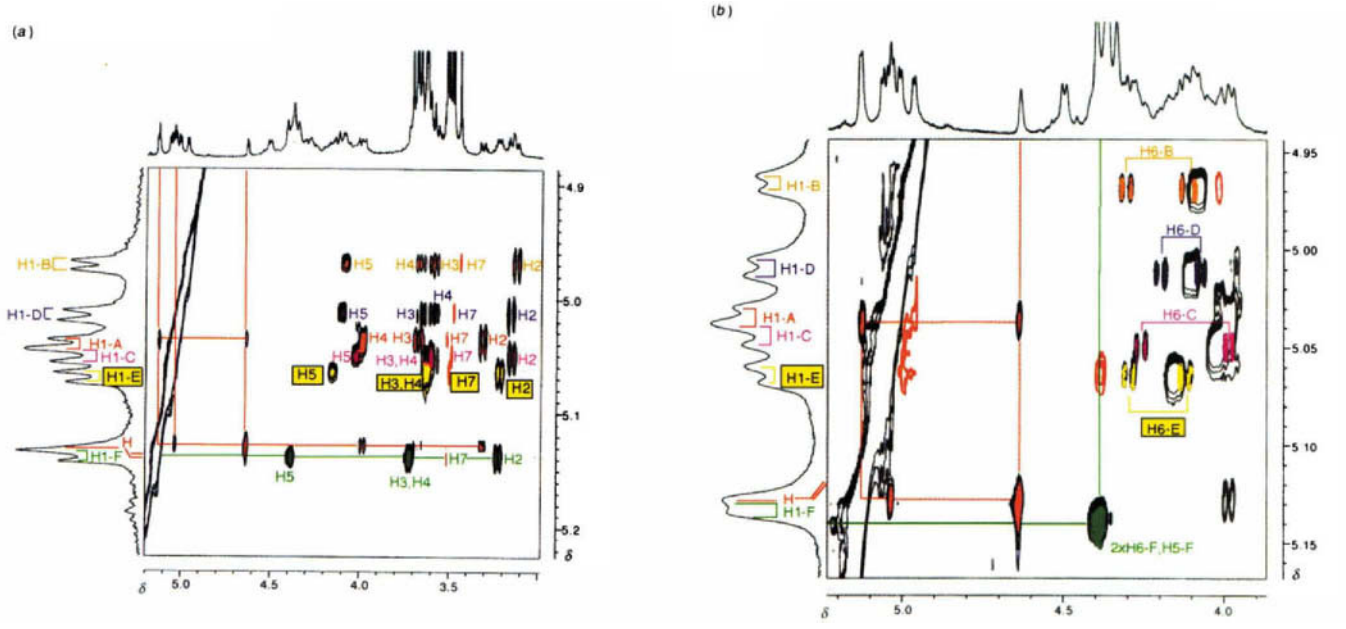

Fig. 4 (*a*) The partial 2D-HOHAHA contour plot for $(4\text{-HMP})_5$-eno-DMαCD, showing an expansion along the H1 rows of the spectrum with the contour levels adjusted to remove the H6 signals for clarity (400 MHz; $CDCl_3$; 22 °C; ref. Me_4Si; 10.4 kHz spin lock field; 150 ms mixing time). (*b*) The partial 2D-HOHAHA contour plot for $(4\text{-HMP})_5$-eno-DMαCD showing an expansion of the H6 signals along the H1 rows of the spectrum (400 MHz; $CDCl_3$; 22 °C; ref. Me_4Si; 10.4 kHz spin lock field; 150 ms mixing time).

totally in agreement with these assignments as additional confirmation.

With regard to the two H6 protons and the H5 proton of ring F (coloured green in the figures), the DQF-COSY data is consistent with total overlap for these signals—this artefact will be shown to be the case when the ^{13}C NMR spectroscopic data are examined later in the discussion section.

The chemical shifts of all the protons of the six pyranosidic protons for $(4\text{-HMP})_5$-eno-DMαCD are presented in Table 1. Using suitable row or column extraction of the 2D-DQF-COSY data, the coupling constants were evaluated as far as was possible without ambiguity. These figures are presented in Table 2.

From an NMR spectroscopy viewpoint, the HOHAHA experiment [10] is interesting, belonging to a family of experiments termed relayed coherence transfer.[11] The coherence is transferred during an isotropic mixing period in the middle of the sequence, the object of which is to provide the efficient suppression of chemical shift terms with energy matching to allow spin exchange. As the duration of the mixing interval increases, the extent to which transfer between coupled spins can occur is enhanced. When long mixing intervals are used, the results are essentially analogous to multistep RELAY experiments. The use of isotropic mixing pulses was first reported by Braunschweiller and Ernst [12] in an experiment given the acronym TOCSY (TOtal Correlation SpectroscopY). When the mixing intervals reach a sufficient length, responses are observed for all members of a spin system, even if they are not directly coupled—hence the acronym given to the experiment.

The HOHAHA sequence uses cross polarisation to transfer coherence between coupled spins in the mixing period.[13] The essential feature of the experiment is the removal of Zeeman contributions [14] during the evolution of the coherence. Once

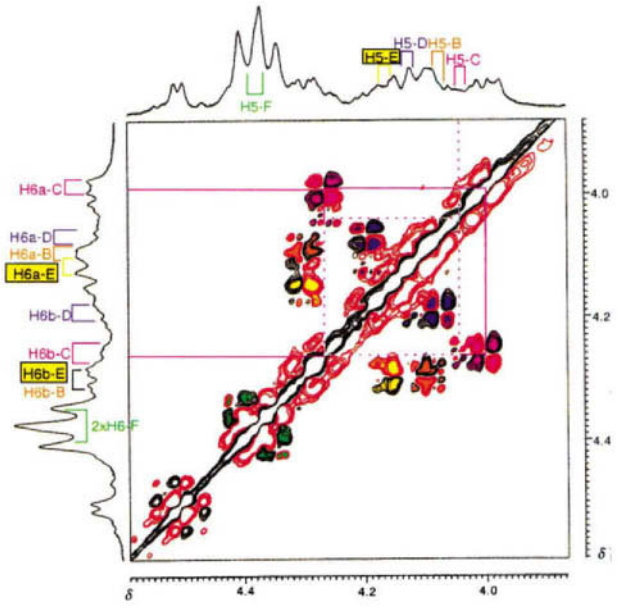

Fig. 5 The partial 2D-DQFCOSY contour plot for (4-HMP)$_5$-eno-DMαCD (400 MHz; $CDCl_3$; 22 °C; ref. Me_4Si) showing the area of the H-6 proton for the five constitutionally heterotopic sugar residues

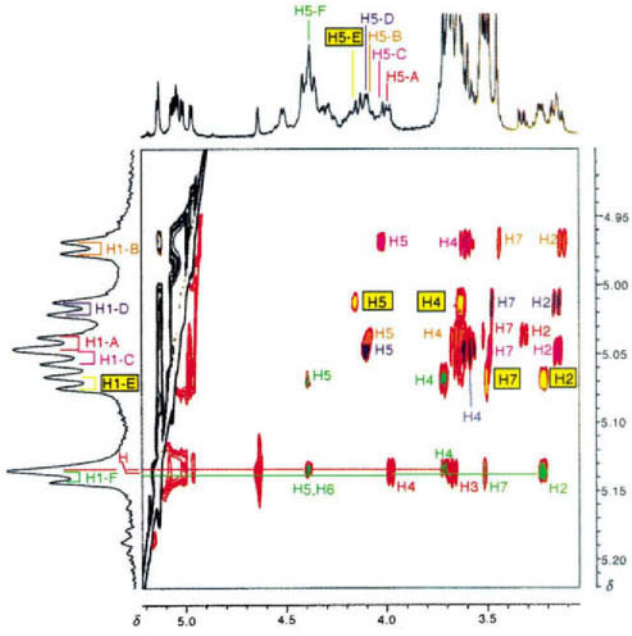

Fig. 6 The partial 2D-ROESY contour plot of (4-HMP)$_5$-eno-DMαCD plotted with a deeper contour level and expanded in the H6 region along the H1 rows (400 MHz; $CDCl_3$; 22 °C; ref. Me_4Si; 2 kHz spin lock field; 100 ms mixing time)

this requirement has been satisfied,[10,15,16] the spin system will evolve under the influence of scalar coupling. Exactly as in the early TOCSY experiment, the duration of the mixing period controls the extent of propagation. Nevertheless, the field of two-dimensional homonuclear relay—whether by scalar coupling or by isotropic mixing—is still in a state of considerable flux and there is much debate as to whether the latter does in fact relay the coherence throughout the spin network in a successive sense.[17]

The chemical shift assignment of (4-HMP)$_5$-eno-DMαCD described earlier is unequivocal on the basis of the long mixing time HOHAHA (150 ms) and the phase-sensitive DQF-COSY experiments. If the HOHAHA experiment is repeated with a shorter mixing period (100 ms), less propagation of the spin system is to be expected. Starting from the anomeric proton round the carbon-only part of the skeleton of the pyranosidic residues, it might be expected that the H5 and H6 protons would not correlate in the projection shown in Fig. 4(*a*). In fact, it is the set of H4 and H6 protons which cease to correlate. This observation implies that the coupling pathway through the ring oxygen atom is equally favourable to HOHAHA transfer even though coupling in a 1D ^1H spectrum is not normally seen between H1 and H5. If both pathways exist, then the H4 and H6 protons are positioned five bonds away from the anomeric proton—the H5 and H3 protons are four bonds from the anomeric protons. Coupling is propagated by way of chemical bonds and so the conservation of orbital symmetry is required for coupling to occur. This effect is potentially the case going from H1 to H4 *via* both the purely carbon skeleton or *via* the ring oxygen atom—all atoms are sp^3 hybridised. If the glycosidic linkage is crossed from H1 to H4, then an eclipsed conformation is observed normally and so, presumably, this breakdown in orbital overlap is why no correlation is observed in the HOHAHA experiment performed with the longer mixing time, *i.e.*, unfavourable orbital overlap.

The observations reported here have done little to alter the opinion regarding the use of isotropic mixing one way or the other. However, what they have done is to highlight the need for careful interpretation of HOHAHA spectra—a point made earlier in the literature by Drobny and co-workers.[18]

HOHAHA data (along with the DQF-COSY data) have led to the identification of the chemical shifts of the ring protons in each of the six different pyranosidic residues in the α-CD. It is now necessary to assign the residue connectivities and one way to achieve this assignment is to identify an nOe cross-peak across the glycosidic linkage between an anomeric proton and the H4 proton on the adjacent pyranosidic residue. Close-contact between the H1 and H4 protons of adjacent pyranosidic residues should be apparent if the pyranosidic residues adopt a $^4C_1$ chair conformation and an eclipsed relationship—H1 to H4—is observable across the glycosidic link.

2D-NOESY experiments were employed under the conditions described in the experimental section but, unfortunately, these experiments failed to provide any meaningful data. 1D-nOe Difference spectroscopy was employed by selectively irradiating each anomeric proton. The sides of the doublet were irradiated with a very low power level to try to obtain the maximum selectivity but no success was achieved. We concluded that the molecular correlation time for the compound was probably such that the sign of the nOe was close to the null point. Accordingly, we resorted to the ROESY experiment, where rOe cross-peaks are always positive, to achieve the residue connectivity information. A partial ROESY spectrum for (4-HMP)$_5$-eno-DMαCD, measured with a mixing time of 100 ms, is reproduced in Fig. 6. In particular, it shows the whole row of cross-peaks for the six anomeric protons. Residue A, coloured red in the figures, and containing the exocyclic double bond, is our starting point. The assignment is started by looking along the row of cross-peaks for the anomeric proton of this residue at δ 5.03 in the $F1$ domain in the ROSEY spectrum. A cross peak into an H4 signal at δ 3.67 and one into an H5 signal at δ 4.09 are clearly visible. From the HOHAHA data, both these signals are consistent with the spin system coloured orange in the figures and so this must be ring B.

Turning attention to the anomeric proton of residue B (the residue coloured orange in the figures), which resonates at δ 4.97, we see that by a similar argument, there exist cross-peaks into an H4 signal occurring at δ 3.62 and an H5 signal at δ 4.02. The HOHAHA data reveals that both of these signals are produced from the protons on the ring system we have designated purple in the figures.

The anomeric proton in the residue C system, now designated purple in the figures, occurs at δ 5.05. This proton shows a cross-peak in the ROESY data to an H4 signal at δ 3.59 and an H5 signal at δ 4.10. HOHAHA data has demonstrated that this signal is part of the spin system designated blue in the figures, *i.e.*, residue D.

The anomeric proton in the ring D system, now designated blue in the figures, occurs at δ 5.01. This proton shows a cross-peak in the ROESY data to an H4 signal at δ 3.63 and an H5 signal at δ 4.16. HOHAHA data has demonstrated that this signal is part of the spin system designated yellow in the figures, *i.e.*, residue E.

The anomeric proton in the ring E system, now designated yellow in the figures, occurs at δ 5.07. This proton shows a cross-peak in the ROESY data to an H4 signal at δ 3.73 and an H5 signal at δ 4.39. HOHAHA data has demonstrated that this signal is part of the spin system designated green in the figures, *i.e.*, residue F.

The cycle is now complete from a colour viewpoint. If the assignment is correct, the anomeric proton (δ 5.14) for the ring F system, designated green in the figures, should show an rOe cross-peak into the H4 resonance of ring A, previously designated red in the figures. A strong cross-peak is clearly visible at δ 3.99. Interestingly, also visible is a cross peak into the H3 resonance of ring A—the ring featuring the exocyclic double bond and which will be distorted as a result.

Also visible in the δ 3.10–3.40 range of the rows of cross-peaks exhibited by the six anomeric protons in the ROESY data are strong rOe peaks into their own respective H2 protons which are also adjacent. Each anomeric proton is clearly in the same ring system as the H2 proton which is giving rise to the rOe cross-peak and the latter is therefore designated the same colour in the figures. The pattern of colour for the H2 protons in the figures in the ROESY data (which originated from spatial considerations), exactly matches the pattern of colour for these same cross-peaks in the HOHAHA data (which originated from coupling considerations).

The row of cross-peaks exhibited by the six anomeric protons in the ROESY data also provides further information in the δ 3.43–3.54 range. A set of closely bunched cross-peaks is evident and is a result of the H7 methoxy protons on the same residue, which, from modelling considerations, are also very close in space to the anomeric protons. The other set of the methoxy protons H8 is not readily assigned. The H8 protons occur in the range δ 3.63–3.71 and all six signals are clearly visible in the 1D spectrum at room temperature. From an examination of models, they are likely to be identified by rOe cross-peaks into H4 or H7. The H8 proton for residue A (the residue coloured red in the figures) is readily identified at δ 3.63 from an rOe cross-peak into H4 on the same residue. Any H8 rOe cross-peaks from the H4 protons are overlapped by the strong HOHAHA cross-peaks into H3 and H4 so further assignment is not immediately evident. The H8 rOe cross-peaks from the H7 protons are in an area of the spectrum clearly affected by T_1 ridges—the methoxy signals are very strong—and again, difficulty in assignment is created. Whilst it may be possible to assign these signals, we would prefer to refrain, given the possibility of error. The absence of their assignment does not detract from our discussion of the conformations of the pyranosidic residues.

The discussion concerning the H6 protons on the exocyclic double bond, which is part of residue A (and coloured red in the figures), has centred around the spin-system demonstrated by the HOHAHA experiments. From a spatial consideration, the ROESY data also clearly demonstrate that the two protons of the AX system are close in space.

Also visible in the ROESY cross-peak data in the anomeric proton area (Fig. 6) is another cross-peak at $\delta \approx 4.4$, which from HOHAHA would be consistent with a signal arising from H5 of residue F (the residue coloured green in the figures). At first glance, this signal appears to originate from the anomeric proton at δ 5.14 (*i.e.*, the anomeric proton of residue F itself—this observation would be a surprising result requiring considerable distortion of the ring). However, closer examination by expanding this region reveals that this unassigned cross-peak, apparently into the H5 resonance of residue F (coloured green in the figures), actually arises from the closely overlapping signal assigned to one of the terminal H6 protons (previously described as the 'A' part of the AX system) of the exocyclic double bond on residue A (coloured red in the figures). Also visible is a further correlation of this exocyclic double bond proton into H4 of residue F and coloured green in the figures. From modelling considerations, for these protons to approach each other directly within rOe contact distance is quite feasible if the exocyclic double bond points into the cavity of the cyclodextrin. The exocyclic H6 protons of the olefin also approach the H6 protons of ring F quite closely. Indeed, we saw earlier in our discussion of the DQF-COSY data that H5 and the two H6 protons appear to overlap almost exactly. The ROESY data would therefore be consistent with cross peaks into either or both resonances. The ^{13}C NMR spectroscopic data provides the confirmation that H5 and the two H6 protons of ring F do, in fact, overlap almost exactly.

The *J*-modulation (JMOD) ^{13}C NMR spectrum of the symmetrical compound 4-HMP-DMαCD is given in Fig. 7(*a*). This spectrum was assigned by 2D C–H correlation spectroscopy and the chemical shifts are listed in Table 3. The C6/H6 correlation cross-peaks were extremely weak but the ^1H AB system is clearly visible in the 2D experiment. The remaining CH_2 signal, evident at $\delta_C \approx 62$, must clearly be assigned to the C13 resonances. The C10 and C11 resonances were assigned by literature precedent.[19]

Fig. 7(*b*) shows the increased complexity of the JMOD ^{13}C NMR spectrum of the unsymmetrical compound $(4\text{-HMP})_5$-eno-DMαCD. This spectrum was assigned by 2D C–H correlation spectroscopy. Again, the C6 carbon atoms did not correlate but, by increasing substantially the number of scans in each increment of the experiment, weak correlations in the C6 area were achieved. A partial contour plot of the C6 area is provided in Fig. 8.

An H6 proton does in fact overlap almost exactly with the H5 proton of residue F (coloured green in the figures) and both signals are further overlapped by signals from H13. The newly found H6 signal must therefore be assigned to residue F. An AB system was expected for the H6 signals possessing a much smaller frequency separation for the A and B protons than has been observed for the other pyranosidic residues. This assignment confirms the DQF-COSY data (Fig. 5) where all cross-peaks in this area of the spectrum appear close to the diagonal. The cross-peaks for the C6/H6 signals in the 2D-CH correlation experiment are clearly very weak and to use them for further assignment of H6 carbons is tentative and unacceptable. The crucial point is that the C–H correlation data confirm the earlier arguments for the H6 protons of residue F (coloured green in the figures).

The reasons why the cross-peaks from C6 to H6 are weak are not clear.[20] The C–H correlation pulse sequence used takes 11.5 ms to complete (an additional 2 s relaxation delay was used). The proton T_1 relaxation times for all the signals in the H6/H4/H13 area under examination are of the order of 0.5 s. Clearly, fast relaxation is not a problem and it is the T_1 relaxation time of the proton (rather than the ^{13}C) that is relevant in this experiment. As a further illustration, the methyl protons in the two methoxy groups on each pyranosidic residue afford good C–H correlations and these have a T_1 relaxation time of 0.9 s. The observation could be caused by fast T_2 relaxation or perhaps,

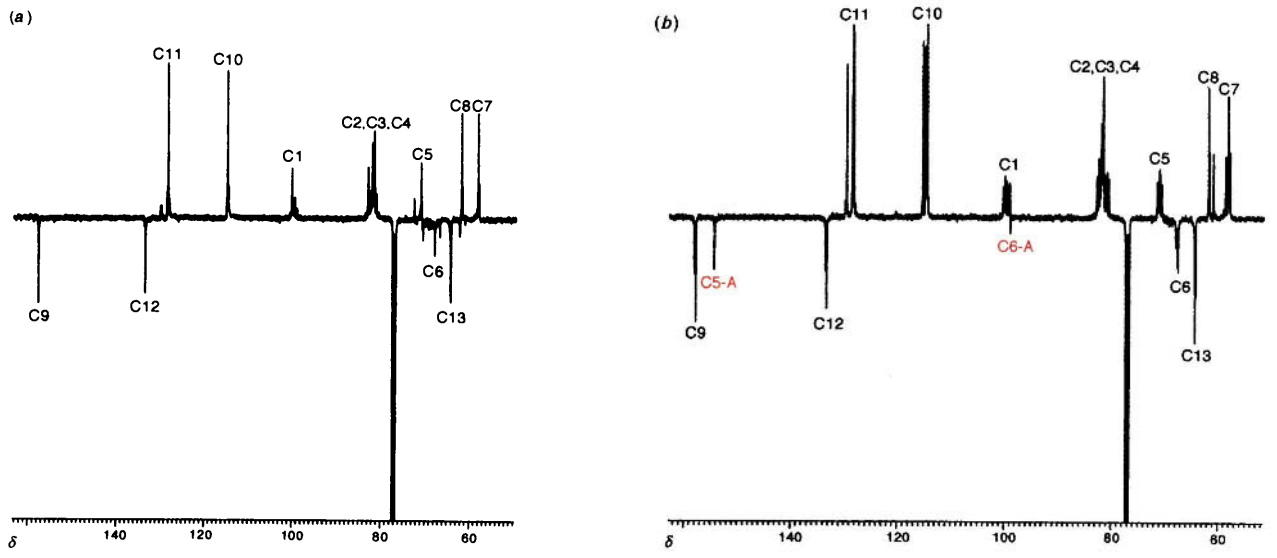

Fig. 7 (*a*) The *J*-modulation spectrum for 4-HMP-DMαCD (100.6 MHz; $CDCl_3$; 22 °C; ref. Me_4Si). (*b*) The *J*-modulation spectrum for $(4\text{-HMP})_5$-eno-DMαCD (100.6 MHz; $CDCl_3$; 22 °C; ref. Me_4Si).

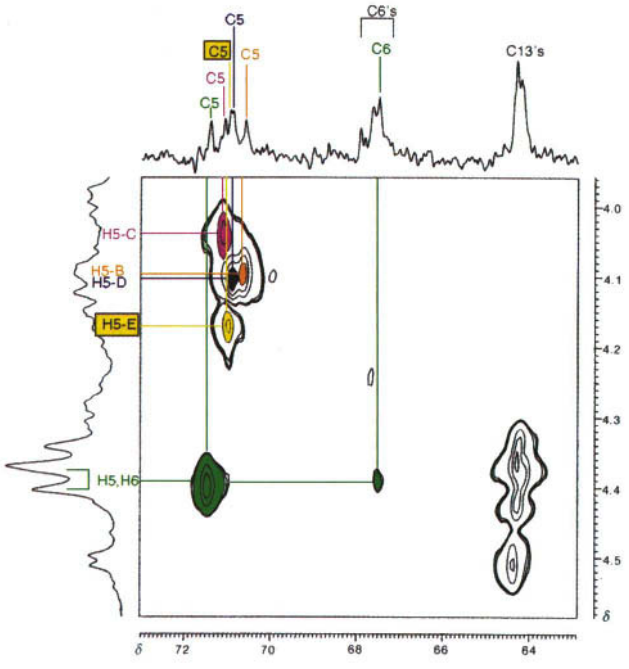

Fig. 8 An expansion of the 2D-CH correlation spectrum for $(4\text{-HMP})_5$-eno-DMαCD showing the H5–C5 and H6–C6 region of the spectrum (400 MHz for ^1H; 100.6 MHz for ^{13}C; $CDCl_3$; 22 °C; ref. Me_4Si)

conformational mobility. The T_2 relaxation times were not measured. In respect of conformational mobility, the aromatic residues attached to the C6 positions on the CD torus induce considerable steric crowding and the CH_2 linkage enables much flexibility. The aromatic residues provide areas of a diamagnetic and paramagnetic shielding and there is every likelihood of fluctuating chemical shifts for these nuclei. To investigate this possibility, the sample was examined by dynamic ^1H NMR spectroscopy. At temperatures of −20 °C, or below, the observed spectrum becomes extremely broad and complex and no assignment was attempted.

The ^{13}C chemical shifts for the unsymmetrical compound $(4\text{-HMP})_5$-eno-DMαCD, are given in Table 3.

A comparison of the ^1H chemical shift data for $(4\text{-HMP})_5$-eno-DMαCD with that of the symmetrical compound 4-HMP-DMαCD (Table 1) shows that the pyranosidic ring protons appear in similar spectral regions. However, there are several different features. For the unsymmetrical compound, five of the anomeric protons are bunched closely together in the δ 4.97 to δ 5.07 range, yet that of anomeric signal ring F (coloured green in the figures), the ring adjacent to ring A, is clearly separate and appears to higher frequency at δ 5.14.

A similar observation holds for the set of H2 protons with five signals bunched close together in the range δ 3.13 to δ 3.33. However, it is the H2 proton from residue A (coloured red in the figures) which is at highest frequency.

The H3 protons for all six pyranosidic residues are also quite close together in the range δ 3.59 to δ 3.68 with the highest frequency signal of the set arising from ring F (coloured green in the figures) once again.

An examination of the H4 chemical shift data for the six pyranosidic rings shows the first, and expected, major deviation from the data observed for the symmetrical compound. Whilst five of the H4 signals lie in the same spectral region as their H3 counterparts, the H4 signal of ring A (coloured red in the figures), featuring the exocyclic double bond, shows a considerable move to higher frequency as a consequence of the olefinic π-electrons.[21] This signal is moved into the region occupied by the H5 resonances of the other five sugar residues. A further point of interest is that, whilst three (rings D, E and F) of the remaining sugar residues exhibit total overlap of their H3 and H4 resonances, as in the symmetrical compound, two (rings B and C) show dispersion. For ring B, H4 resonates slightly to higher frequency of its H3 counterpart. In the case of ring C, the opposite is observed.

As regards the H5 protons, those for four of the pyranosidic rings resonate in a similar region of the spectrum (δ 4.02 to δ 4.16), corresponding to the range that is observed for the symmetrical compound. However, one of the H5 resonances (that of ring F, coloured green in the figures) appears at considerably higher frequency than the rest at δ 4.73. (It will be recalled that there are only five H5 signals because that of ring A has undergone elimination.) Ring F is adjacent to ring A. As already described, the ROESY data show an rOe cross-peak from H5 of ring F into an H6 proton of ring A. The close spatial proximity of the H5 proton to the π-electrons of the exocyclic double bond could be the reason for this lower chemical shift value compared with those for the H5 protons of the other residues.

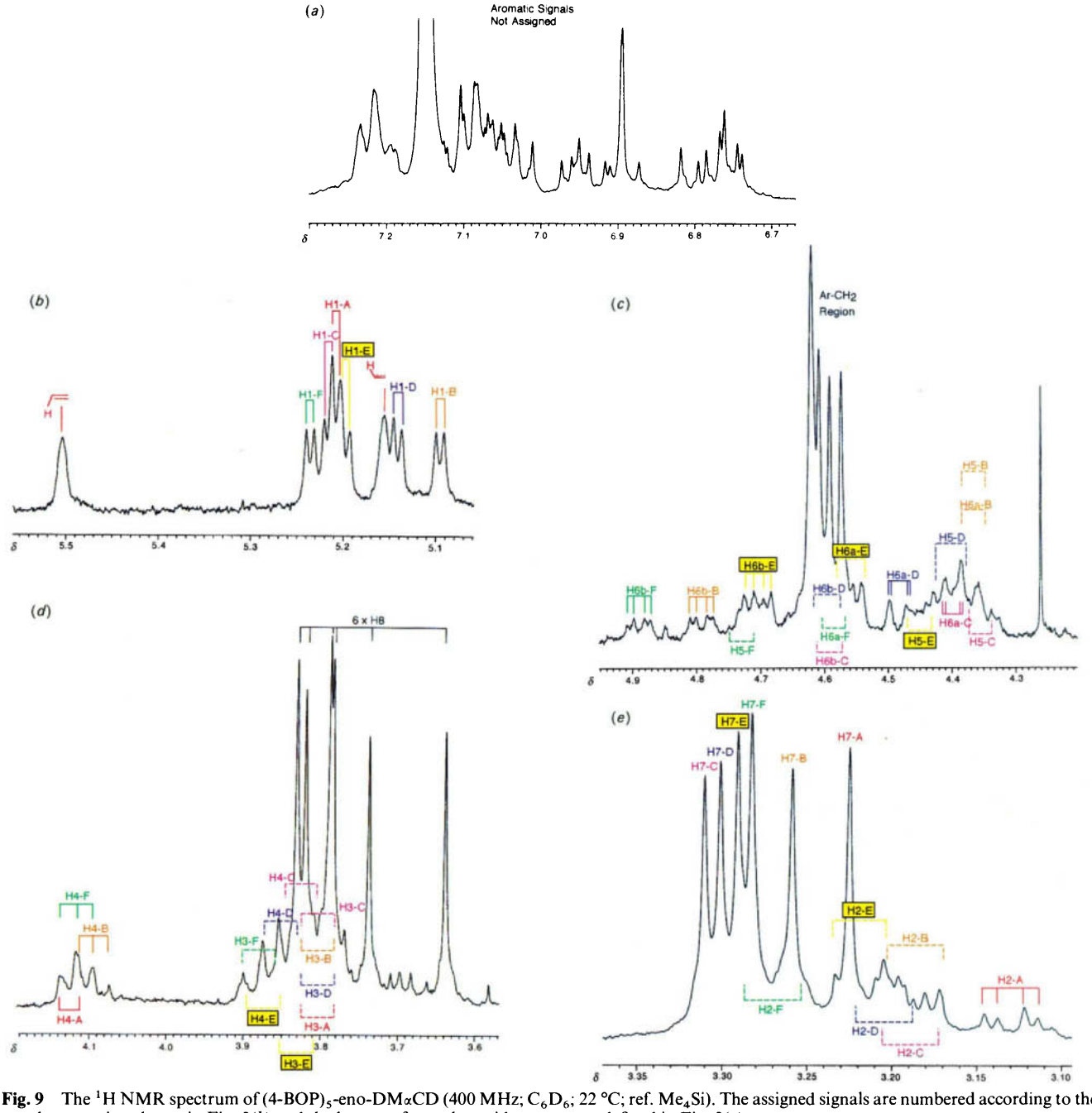

Fig. 9 The ^{1}H NMR spectrum of (4-BOP)$_5$-eno-DMαCD (400 MHz; C_6D_6; 22 °C; ref. Me_4Si). The assigned signals are numbered according to the usual convention shown in Fig. 3(*b*) and the letters refer to the residue sequence defined in Fig. 3(*a*).

The ^{13}C NMR spectroscopic data for the unsymmetrical (4-HMP)$_5$-eno-DMαCD compound shows that the carbon atoms resonate in similar spectral regions to their counterparts in the symmetrical 4-HMP-DMαCD compound (Table 3). Note, however, that C5 in ring A, which is now olefinic in nature, resonates at δ 154.3 unlike the five sp^3-hybridised carbon atoms of the other five pyranosidic residues which appear around δ 71.

The ROESY data (Fig. 6) allow some further insight into the solution structure. If ring A (coloured red in the figures) is taken as the starting point, the anomeric proton of this ring shows rOe cross peaks into H4 and H5 of the adjacent ring B. This observation pattern is the case for rings B, C, D and E. However, the anomeric proton of ring F (coloured green in the figures) shows rOe cross peaks into H4 and H3 of ring. A.

An examination of CPK space-filling molecular models and computer-aided molecular modelling shows that the introduction of the double bond at position C5 in ring A does introduce considerable distortion into the pyranose ring. Modelling suggests that the effect of incoporation of the exocyclic double bond is to cause a 'flattening' of the residue. As a consequence of this localised distortion, the torus of the CD is forced into an unsymmetrical conformation, where at least one of the glycosidic linkages is puckered.

The full ^{1}H NMR spectral assignment of the similarly unsymmetrical and related compound (4-BOP)$_5$-eno-DMαCD recorded in C_6D_6 at room temperature has also been achieved. The same colour scheme for the residue connectivities as described for the (4-HMP)$_5$-eno-DMαCD compound in Fig. 3 was maintained for the (4-BOP)$_5$-eno-DMαCD spectra. Fig. 3 also shows the numbering system used. The ^{1}H NMR spectrum is shown in Fig. 9(*a*)–(*e*) and, as before, we have not assigned any of the aromatic protons for the 4-BOP group at position 6. The spectral assignments were once again made from

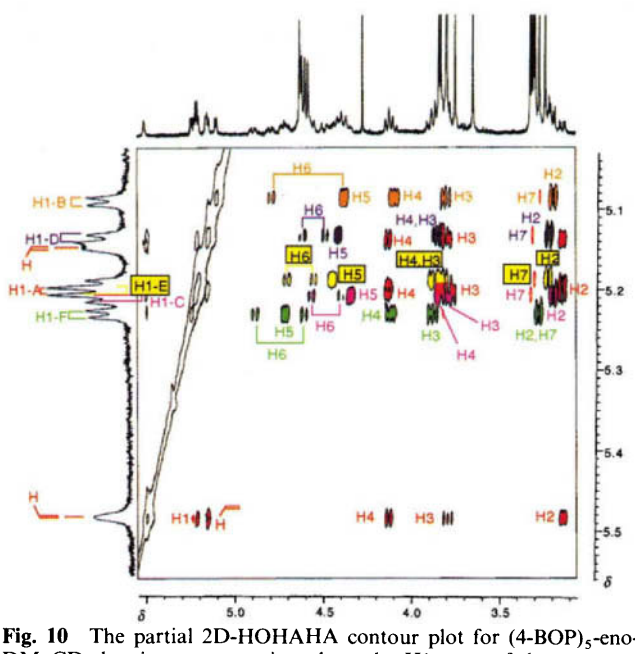

Fig. 10 The partial 2D-HOHAHA contour plot for $(4\text{-BOP})_5$-eno-DMαCD showing an expansion along the H1 rows of the spectrum (400 MHz; C_6D_6; 22 °C; ref. Me_4Si; 10.4 kHz spin lock field; 150 ms mixing time)

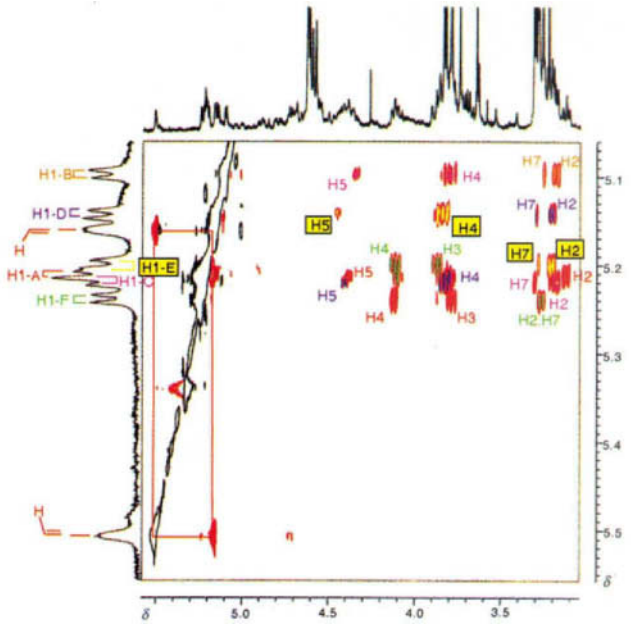

Fig. 11 The partial 2D-ROESY contour plot for $(4\text{-BOP})_5$-eno-DMαCD showing an expansion along the H1 rows (400 MHz; C_6D_6; 22 °C; ref. Me_4Si; 2 kHz spin lock field, 100 ms mixing time)

Table 4 ^{1}H NMR chemical shifts (ppm) for $(4\text{-BOP})_5$-eno-DMαCD[a] (400 MHz; C_6D_6; 22 °C)

	$(4\text{-BOP})_5$-eno-DMαCD					
Proton	A	B	C	D	E	F
H-1	5.20	5.09	5.21	5.14	5.20	5.23
H-2	3.14	3.19	3.19	3.21	3.22	3.27
H-3	3.78	3.80	3.78	3.81	3.81	3.87
H-4	4.11	4.09	3.83	3.85	3.87	4.11
H-5	N/A	4.38	4.34	4.40	4.44	4.70
H-6a[b]	5.15	4.38	4.39	4.48	4.54	4.87
H-6b[b]	5.49	4.78	4.56	4.60	4.70	4.60
H-7	3.22	3.26	3.31	3.30	3.29	3.29

[a] The residues are labelled according to Fig. 3. [b] H6a and H6b can be identified from coupling considerations.[34,35]

HOHAHA, DQF-COSY and ROESY spectra, exactly as described earlier for the $(4\text{-HMP})_5$-eno-DMαCD compound. The rows of cross peaks for the six anomeric protons in the partial HOHAHA spectrum are shown in Fig. 10. The conditions of the experiment once again allowed the correlations for all seven protons of the respective pyranosidic spin systems to be observed (six in the case of ring A). Also, there is very little spectral overlap and the assignment is straightforward. As described earlier, for $(4\text{-HMP})_5$-eno-DMαCD, when performing the HOHAHA experiment with a reduced mixing period (100 ms), the 'loss' of the H4 and the H6 protons is observed. The H5 protons remain in the spectrum as was noted for the $(4\text{-HMP})_5$-eno-DMαCD analysis. The chemical shift data is presented in Table 4.

The ROESY data established the ring connectivity and the rows of cross peaks for the six anomeric protons in the partial ROESY spectrum is shown in Fig. 11. The DQF-COSY data clearly show the H5/H6 connectivity in Fig. 12 and suitable row and column extraction yielded the coupling constant data. These data are presented in Table 5.

In the absence of data for the symmetrical counterpart of $(4\text{-BOP})_5$-eno-DMαCD, comparisons with the ^{1}H NMR spectroscopic data for $(4\text{-HMP})_5$-eno-DMαCD will be described but it must be realised that the data for the former

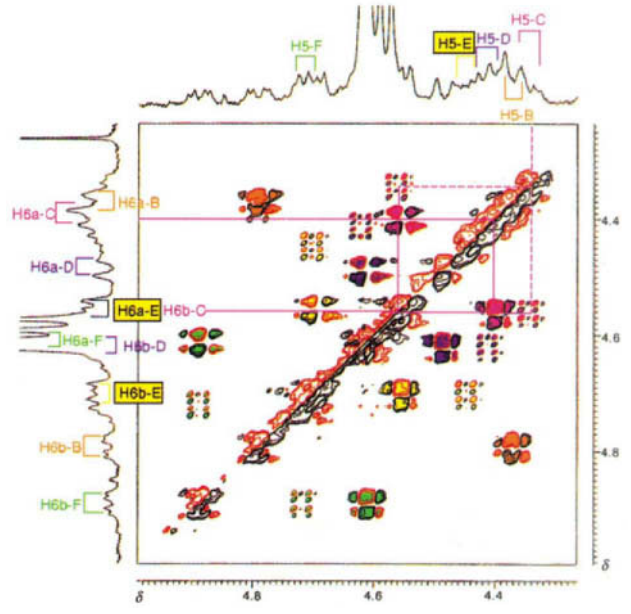

Fig. 12 The partial 2D-DQFCOSY contour plot for $(4\text{-BOP})_5$-eno-DMαCD (400 MHz; $CDCl_3$; 22 °C; ref. Me_4Si) showing the area of the H6 protons for the five constitutionally heterotopic sugar residues

compound (Table 4) were obtained in C_6D_6, whilst that for the latter (Table 1) was obtained in $CDCl_3$.

The data are very similar. Certainly, all the pyranosidic ring protons resonate in the same spectral regions for both compounds. However, the signals for the anomeric protons show less dispersion and exhibit a different dispersion pattern—note the slightly different order for the spin systems coloured purple and red in Figs. 4 and 10 in the respective HOHAHA spectra even though, as has been stated, the colour sequence for the sugar ring connectivity, as drawn in Fig. 3, is the same for both compounds. Ring A, coloured red in the figures, is the starting point for both analyses.

Unlike the analysis of $(4\text{-HMP})_5$-eno-DMαCD, where the H2 proton for ring A was the highest frequency signal of the H2 set of signals, the H2 proton for ring A in $(4\text{-BOP})_5$-eno-DMαCD

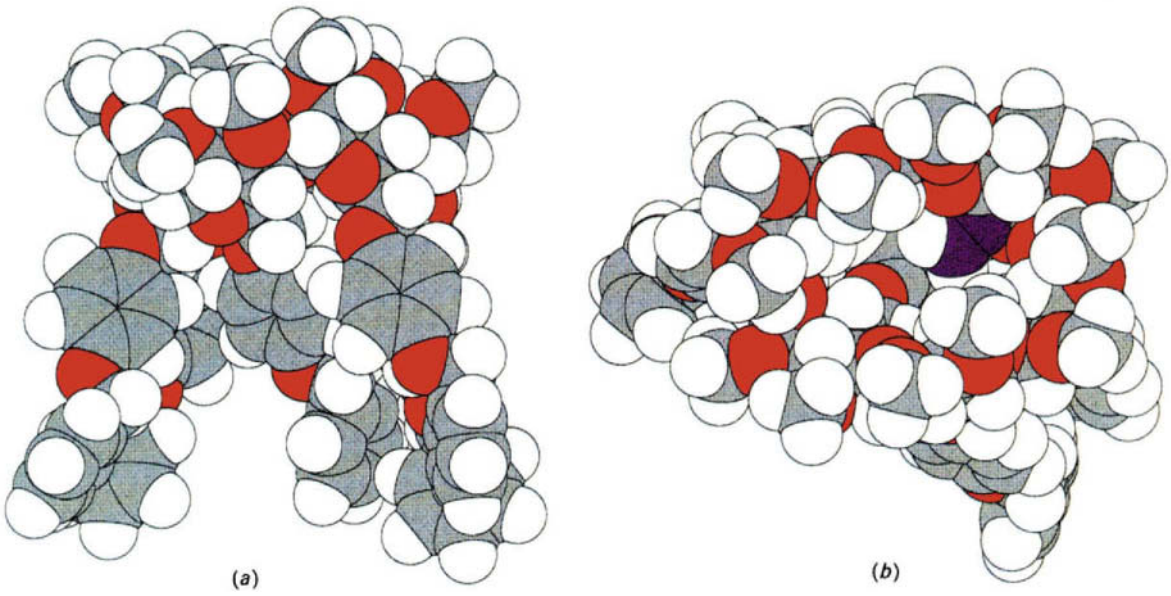

Fig. 13 (*a*) Space filling representation of the calculated structure (MM3*) of (4-BOP)$_5$-eno-DMαCD, side projection. (*b*) Space filling representation of the calculated structure (MM3*) of (4-BOP)$_5$-eno-DMαCD viewed from the secondary face of the CD. The exocyclic double bond located on ring A is highlighted in blue.

Table 5 Coupling constants[a] (Hz) for (4-BOP)$_5$-eno-DMαCD

	(4-BOP)$_5$-eno-DMαCD[b]					
$^3J_{H,H}$	A	B	C	D	E	F
$^3J_{1,2}$	4.0	4.0	4.0	4.0	4.0	4.0
$^3J_{2,3}$	10.0	10.0	10.0	9.0	10.0	10.0
$^3J_{3,4}$	9.0	8.0	8.0	9.0	8.0	8.0
$^3J_{4,5}$	N/A	10.0	10.0	10.0	10.0	10.0
$^3J_{5,6a}$[c]	N/A		Not accessible			
$^3J_{5,6b}$[c]	N/A	5.0	5.0	5.0	5.0	5.0
$^3J_{6a,6b}$	Broad	11.0	11.0	11.0	11.0	11.0

[a] The data are taken from the DQFCOSY spectrum (400 MHz; C_6D_6; 22 °C). The coupling constants were measured and rounded to the nearest integer to respect the digitisation limits of the experiment. [b] The residues are labelled according to Fig. 3. [c] See refs. 34 and 35.

is now the lowest frequency signal of the set. All the H2 signals, though well dispersed, do occur in a narrow δ range.

There is more dispersion in the H3 and H4 signal area for (4-BOP)$_5$-eno-DMαCD and, in every case, H4 resonates to higher frequency than H3. Interestingly, H4 of ring A would once again be expected to show the lowest field signal of the set of H4 protons because of the effect of the olefinic π-electrons. This prediction is indeed the case but the H4 protons for both ring B (coloured orange in the figures) and ring F (coloured green in the figures) resonate almost at a similarly low chemical shift to that of ring A. This spectral artefact was not observed for the (4-HMP)$_5$-eno-DMαCD compound where the H4 proton of ring A in this situation was quite alone. It is worthwhile restating that ring B and ring F are positioned either side of ring A, which features the exocyclic double bond.

For the (4-BOP)$_5$-eno-DMαCD compound, the H5 protons are observed to markedly higher frequency of the H4 protons. [The H4 proton of ring A did overlap the H5 proton area for the (4-HMP)$_5$-eno-DMαCD compound.]

Once again, as was observed for (4-HMP)$_5$-eno-DMαCD, it is the H5 proton of ring F, the ring adjacent to ring A, that occurs markedly to higher frequency of the rest.

In the (4-BOP)$_5$-eno-DMαCD compound, all the H6 protons show wide AB frequency dispersion. It will be recalled in particular that H5 and the two H6 protons of ring F (coloured green in the figures), showed complete overlap in the (4-HMP)$_5$-eno-DMαCD case.

The ROESY data for the (4-BOP)$_5$-eno-DMαCD compound show similarity to those described earlier for (4-HMP)$_5$-eno-DMαCD. It will be recalled that for this latter compound, residues A to E showed a correlation between the anomeric proton and H5/H4 of the adjacent residue. The anomeric proton of residue F, which is adjacent to the starting point (residue A) showed a correlation with H4 and H3—H5 does not exist for ring A, having been eliminated.

For (4-BOP)$_5$-eno-DMαCD, the anomeric protons of residues A to D showed correlations with H5/H4, as described above, but those of residues E and F showed correlations with H4/H3. Residue E, in principle, does have the possibility to correlate with H5 of residue F but this possibility was not observed. Again, the ROESY data were able to confirm the accurate chemical shifts of the H7 protons.

In order to gain a more accurate picture of the solution phase structure of (4-BOP)$_5$-eno-DMαCD, a series of molecular mechanics calculations was carried out on this molecule using the MM3* forcefield[22] and the GB/SA solvation model of Still and co-workers[23] for $CHCl_3$. Full details of these calculations can be found in the experimental section. The results indicate (Fig. 13) that the molecule has a reasonably open structure with the pendant (4-benzyloxy)phenyl ether groups extending away from the cyclodextrin torus. The cyclodextrin torus itself has undergone significant distortion as a result of the introduction of a double bond into one of the glucopyranose rings. Calculation of coupling constants from the minimum energy structure for (4-BOP)$_5$-eno-DMαCD reveals values (Table 6), which are in good agreement with the experimental values (Table 5)—the values obtained from the calculated structure are within the experimental error—indicating that the calculated structure portrays the conformations of the individual glucopyranoside residues accurately. The calculated structure also correctly predicts the rOe observed between one H6 on the double bond and the H5 of the adjacent F ring (green). There is also good agreement between close contacts in the calculated structure and experimentally observed rOe data. Interestingly, four anomeric protons show close contacts with H4/H5's of adjacent rings and two, namely those of ring F and B, showed close contacts for H4/H3.

Table 6 Coupling constants (Hz) calculated[a] for the minimum-energy structure for (4-BOP)$_5$-eno-DMαCD

	(4-BOP)$_5$-eno-DMαCD[b]					
$^3J_{H,H}$	A	B	C	D	E	F
$^3J_{1,2}$	2.9	2.7	3.3	3.0	2.9	3.3
$^3J_{2,3}$	9.9	9.6	9.9	9.5	9.6	9.8
$^3J_{3,4}$	8.7	7.7	9.0	8.6	7.9	9.1
$^3J_{4,5}$	—	8.5	9.5	9.4	9.0	9.6

[a] C. A. G. Haasnoot, F. A. A. M. De Leeuw and C. Altona, *Tetrahedron*, 1980, **36**, 2783. [b] The residues are labelled according to Fig. 3.

Conclusions

The detailed investigation reported in this paper has demonstrated that mass spectrometry, NMR spectroscopy—employing modern pulse sequences—and computer molecular modelling are indispensible tools for elucidating the structural characteristics of complex unsymmetrical cyclodextrin molecules.

If we exclude the H8 methoxy resonances and all the signals originating from the aromatic substituents at the C6 position from the analyses, the (4-HMP)$_5$-eno-DMαCD and (4-BOP)$_5$-eno-DMαCD derivatives each contain 59 heterotopic protons and 42 heterotopic carbon atoms. Both of these compounds have been subjected to a total ^{1}H NMR spectroscopic assignment. Additionally, for (4-HMP)$_5$-eno-DMαCD the methoxy proton for H8 of residue A (coloured red in the figures) has been identified.

For (4-HMP)$_5$-eno-DMαCD, the 2D C–H correlation experiment has allowed us to assign all of the 42 heterotopic carbon atoms, except for four C-6 carbon atoms from the constitutionally similar pyranosidic residues.

The studies presented here have demonstrated that the task of isolating and fully characterising unsymmetrical chemically modified CDs is not insurmountable. We stress the importance of characterising such compounds, to very high tolerances, since it is imperative that their structures are shown to be unambiguous on account of the large number of possible structures that can be generated when modifying cyclodextrins. Further, a full characterisation in terms of NMR spectroscopic parameters is essential if the binding properties of modified cyclodextrins are to be investigated in detail.

Experimental

α-CD (Wacker) and all reagents (Aldrich) were used as received. All solvents were dried according to standard laboratory practice before being used. Thin layer column chromatography (TLC) was performed on Silica Gel 60 F_{254} aluminium plates (Merck 5554) and reversed-phase TLC was performed on Silica Gel RP-8 F_{254}s glass plates (Merck 15684). Column chromatography was performed on Silica Gel 60 (Merck 9385). Melting points were determined with an Electrothermal 9200 apparatus. Reversed-phase high performance liquid chromatography was performed on a Gilson Gradient HPLC System, equipped with an Anachem reversed-phase C_{18} 60A column using Gilson 715 HPLC System Controller Software and a Rainin Dynamax UV-1 variable wavelength UV–VIS absorbance detector set at 270 nm.

Hexakis(2,3-di-*O*-methyl)-α-cyclodextrin

Hexakis(2,3-di-*O*-methyl-6-*O*-TBDMS)-α-cyclodextrin[6] (6.10 g, 3.34 mmol) was dissolved in the minimum amount of dry tetrahydrofuran (150 cm^3) under a nitrogen atmosphere. Tetrabutylammonium fluoride hydrate (1 molar solution in tetrahydrofuran, 22.0 cm^3, 22.0 mmol) was added to the solution and the mixture stirred at room temperature for 6 h. The reaction was monitored by TLC (acetone–hexane 25:75 v/v) until one component was observed just above the base line and all faster migrating components had disappeared. The solvent was then removed under reduced pressure to afford a brown mobile oil. The oil was dissolved in water (100 cm^3) and washed with hexane (2 × 75 cm^3). The aqueous layer was collected and passed through a column containing cationic exchange resin (Amberlite IRA-400) and the resulting colourless solution collected over K_2CO_3 (0.50 g). The solvent was removed under reduced pressure to yield a white solid which was dissolved in dichloromethane (50 cm^3) and filtered through Hiflo filter aid. The solvent was removed under reduced pressure to afford a white solid characterised as **hexakis(2,3-di-*O*-methyl)-α-cyclodextrin** (3.60 g, 95%). Mp = 200–201 °C; *m/z* (positive ion FABMS) 1163 ([M + Na]$^+$ for $C_{48}H_{84}O_{30}$); δ_H(400 MHz; D_2O) 3.15 (6 H, dd, $^3J_{1,2}$ = 3.5, $^3J_{2,3}$ = 9.5 Hz, H-2), 3.32 (18 H, s, 2-OCH$_3$), 3.44 (18 H, s, 3-OCH$_3$), 3.51–3.55 (12 H, 2 × dd, H-3 and H-4), 3.63 (6 H, m, H-5), 3.68 (6 H, dd, $^3J_{6a,5}$ = 2.0, $^3J_{6a,6b}$ = 12.5 Hz, H-6a), 3.74 (6 H, dd, $^3J_{6b,5}$ = 4.0, $^3J_{6b,6a}$ = 12.5 Hz, H-6b), 5.06 (6 H, d, $^3J_{1,2}$ = 3.5 Hz, H-1); δ_C(100.6 MHz; D_2O) 60.2 (2-OCH$_3$), 62.6 (3-OCH$_3$), 63.2 (C-6), 74.4 (C-5), 81.7 (C-3), 82.6 (C-2), 83.4 (C-4), 100.3 (C-1).

Hexakis(2,3-di-*O*-methyl-6-deoxy-6-iodo)-α-cyclodextrin

Dry triphenylphosphine (8.00 g, 0.305 mol) was dissolved in dimethylformamide (100 cm^3) and iodine (8.00 g, 0.315 mol) was added portionwise with care and cooling using an external water bath at 15 °C over a period of 30 min. The resulting dark brown solution was allowed to warm to room temperature with stirring over 1 h and hexakis(2,3-di-*O*-methyl)-α-cyclodextrin (2.00 g, 1.75 mmol) was added. The reaction was stirred at 65 °C for 12 h under a nitrogen atmosphere. The dimethylformamide was removed under reduced pressure at 65 °C to afford a viscous brown oil which was dissolved in ethyl acetate (100 cm^3) and washed twice with water (75 cm^3). The organic layer was dried ($MgSO_4$) and the solvent was removed under reduced pressure to afford a brown oil which crystallised on standing. The solid was subjected to column chromatography on silica gel (acetone–hexane 40:60 v/v) to afford pure fractions of a white fluffy solid characterised as **hexakis(2,3-di-*O*-methyl-6-deoxy-6-iodo)-α-cyclodextrin** (2.10 g, 65%). Mp = 270 °C (decomp.) (Found: [M + Na]$^+$ 1822.9377. $C_{48}H_{78}I_6NaO_{24}$ requires 1822.9049); δ_H(400 MHz; C_6D_6) 3.03 (6 H, dd, $^3J_{2,1}$ = 3.5, $^3J_{2,3}$ = 9.5 Hz, H-2), 3.19 (18 H, s, 2-OCH$_3$), 3.39 (6 H, dd, $^3J_{4,3}$ = 8.5, $^3J_{4,5}$ = 8.5 Hz, H-4), 3.52 (6 H, dd, $^3J_{3,4}$ = 8.5, $^3J_{3,2}$ = 9.5 Hz, H-3), 3.61 (18 H, s, 3-OCH$_3$), 3.67 (6 H, m, H-5), 3.82 (6 H, dd, $^3J_{6b,5}$ = 5.0, $^3J_{6b,6a}$ = 11.0 Hz, H-6b), 3.87 (6 H, dd, $^3J_{6a,5}$ = 2.5, $^3J_{6a,6b}$ = 11.0 Hz, H-6a), 5.00 (6 H, d, $^3J_{1,2}$ = 3.5 Hz, H-1); δ_C(100.6 MHz; C_6D_6) 10.0 (C-6), 57.8 (2-OCH$_3$), 61.6 (3-OCH$_3$), 71.2 (C-5), 80.8 (C-3), 82.4 (C-2), 86.7 (C-4), 99.6 (C-1).

$2^A,2^B,2^C,2^D,2^E,2^F,3^A,3^B,3^C,3^D,3^E,3^F$-Dodeca-*O*-methyl-$6^A,6^B,6^C,6^D,6^E,6^F$-hexa-*O*-(4-hydroxymethylphenyl)-α-cyclodextrin and 6^A-deoxy-$5^A,6^A$-didehydro-$2^A,2^B,2^C,2^D,2^E,2^F,3^A,3^B,3^C,3^D,3^E,3^F$-dodeca-*O*-methyl-$6^B,6^C,6^D,6^E,6^F$-penta-*O*-(4-hydroxymethylphenyl)-α-cyclodextrin

4-Hydroxybenzyl alcohol (0.69 g, 5.56 mmol) was added to a suspension of K_2CO_3 (3.80 g, 0.03 mol) in dry acetonitrile (100 cm^3) under a nitrogen atmosphere and stirred for 2 h to afford a lilac coloured suspension. Hexakis(2,3-di-*O*-methyl-6-deoxy-6-iodo)-α-cyclodextrin (0.50 g, 0.28 mmol) was added and the reaction stirred at 80 °C for a period of 2 weeks while being monitored by analytical HPLC using an Anachem 60A reversed-phase C_{18} column and gradient elution (water–acetonitrile 25:75 v/v to pure acetonitrile over a period of 5 min

with a flow rate of 2 cm^3 min^{-1}). After completion of the reaction, the suspension was filtered through a small pad of Hiflo filter aid. The filtrate was collected and the solvent was removed under reduced pressure. The resulting pale brown solid was sonicated in chloroform (75 cm^3) and filtered through a small pad of Hiflo filter aid to give a pale yellow solution. The solvent was removed under reduced pressure to yield a pale yellow solid which was analysed by positive ion FABMS to reveal two main peaks m/z = 1799 $[M + Na]^+$ and 1676 $[M + Na]^+$. The solid was then subjected to preparative HPLC using an Anachem 60A reversed-phase C_{18} column and gradient elution (water–acetonitrile 25:75 v/v to pure acetonitrile over a period of 5 min with a flow rate of 20 cm^3 min^{-1}) to give two compounds characterised as **hexakis[2,3-di-*O*-methyl-6-*O*-(4-hydroxymethylphenyl)]-α-cyclodextrin** (35 mg, 7%), mp 159–162 °C (Found: $[M + Na]^+$ 1799.7457. $C_{90}H_{120}O_{36}Na$ requires 1799.7542); δ_H(400 MHz; $CDCl_3$; 50 °C) 3.20 (6 H, dd, $^3J_{2,1}$ = 4.0, $^3J_{2,3}$ = 9.5 Hz, H-2), 3.52 (18 H, s, 2-OCH_3), 3.66 (12 H, H-3, H-4), 3.65 (18 H, s, 3-OCH_3), 4.18 (12 H, H-5, H-6a), 4.32 (6 H, dd, $^3J_{6b,5}$ = 4.5, $^3J_{6b,6a}$ = 10.5 Hz, H-6b), 4.35 (12 H, s, H-13), 5.01 (6 H, d, $^3J_{1,2}$ = 4.0 Hz, H-1), 6.51 (12 H, d, $^3J_{10,11}$ = 8.5 Hz, H-10), 6.88 (12 H, d, $^3J_{11,10}$ = 8.5 Hz, H-11); δ_C($CDCl_3$; 100.6 MHz) 58.1 (2-OCH_3), 61.9 (3-OCH_3), 64.5 (C-13), 67.9 (C-6), 71.0 (C-5), 81.6 (C-3), 82.0 (C-2), 82.9 (C-4), 100.1 (C-1), 114.9 (C-11), 128.4 (C-10), 133.5 (C-9), 157.9 (C-12) and **6^A-deoxy-5^A,6^A-didehydro-2^A,2^B,2^C,2^D,2^E,2^F,3^A,3^B,3^C,3^D,3^E,3^F-dodeca-*O*-methyl-6^B,6^C,6^D,6^E,6^F-penta-*O*-(4-hydroxymethylphenyl)-α-cyclodextrin** (90 mg, 20%) (Found: $[M + Na]^+$ 1675.6933. $C_{83}H_{112}NaO_{34}$ requires 1675.6679).

6^A-Deoxy-5^A,6^A-didehydro-2^A,2^B,2^C,2^D,2^E,2^F,3^A,3^B,3^C,3^D,3^E,3^F-dodeca-*O*-methyl-6^B,6^C,6^D,6^E,6^F-penta-*O*-(4-benzyloxyphenyl)-α-cyclodextrin

4-Benzyloxyphenol (1.11 g, 5.56 mmol) was added to a suspension of K_2CO_3 (3.80 g, 0.03 mol) in dry acetonitrile (100 cm^3) under a nitrogen atmosphere and stirred for 2 h until the suspension was purple in colour. Hexakis(2,3-di-*O*-methyl-6-deoxy-6-iodo)-α-cyclodextrin (0.50 g, 0.28 mmol) was added and the reaction was stirred at 80 °C while being monitored by positive-ion FABMS for m/z 2255. After 1 week the reaction mixture was filtered through a small pad of Hiflo super-cel filter aid. The filtrate was collected and the solvent was removed under reduced pressure. The resulting yellow solid was sonicated in chloroform (75 cm^3) and filtered through a small pad of Hiflo super-cell filter aid to give a pale yellow solution. The solvent was removed under reduced pressure to yield a pale yellow solid which was analysed by positive-ion FABMS to reveal a peak m/z = 2055 $[M + Na]^+$. The solid was then subjected to preparative HPLC using an Anachem 60A reversed-phase C_{18} column and gradient elution (water–acetonitrile 25:75 v/v to pure acetonitrile over a period of 5 min with a flow rate of 20 cm^3 min^{-1}) to give a white solid characterised as **6^A-deoxy-5^A,6^A-didehydro-2^A,2^B,2^C,2^D,2^E,2^F,3^A,3^B,3^C,3^D,3^E,3^F-dodeca-*O*-methyl-6^B,6^C,6^D,6^E,6^F-penta-*O*-(4-benzyloxyphenyl)-α-cyclodextrin** (35 mg, 6%) (Found: $[M + Na]^+$ 2055.8498. $C_{113}H_{132}NaO_{34}$ requires 2055.8617).

Computational studies

Molecular mechanics calculations using the MM3* forcefield and the GB/SA solvation model[23] for $CHCl_3$ were carried out using the Macromodel 4.0x program running on Silicon Graphics Indy, Iris Indigo, or Personal Iris 4D/35TG workstations. An initial input structure for (4-BOP)$_5$-eno-DM-α-cyclodextrin was constructed by appropriate modification of and addition to the X-ray crystal structure of α-CD solved by Saenger and co-workers.[24] This initial structure was minimised using the Polak–Ribière conjugate gradient method and a series of minimum energy structures were then located by pseudo Monte Carlo conformational searching (2000 step searches repeated four times from different starting geometries). The ten lowest energy structures from these searches were then minimised using the Newton–Raphson method to give the structure shown in Fig. 13 as the lowest energy conformation.

For comparison purposes, gas-phase calculations were carried out using the CHARMm forcefield, through Quanta interface,[25] running on a Silicon Graphics Iris Indigo workstation. Conformation searching was carried out using the random sampling method (1600 step searches, 40 torsion angles varied, torsion angle window 60°, repeated four times). The ten lowest energy conformations from these searches were treated as above and gave results which were broadly similar to the solution phase calculations, although the pendant (4-benzyloxy)phenyl ether groups had much less extended conformations.

Mass spectrometry

Low resolution fast atom bombardment mass spectra (FABMS) were obtained using a Kratos MS80RF mass spectrometer (accelerating voltage, 3 kV; resolution 1000) coupled to a DS90 data system and off-line Sun workstation for processing the raw data experiments. The atom gun was an adapted saddle field source (Ion Tech. Ltd.) operated at 8 kV and a tube current of about 2 mA. Krypton was used to provide a primary beam of atoms and samples were dissolved in a small volume of 3-nitrobenzyl alcohol that had been previously coated onto a stainless steel probe tip. Spectra were recorded as raw data in the positive-ion mode at a scan speed of 10 s per decade prior to summation and processing. It was found that the addition of trace amounts of sodium acetate to the matrix promoted cationisation of the sample and led to a considerable improvement in the signal strength of the $[M + Na]^+$ pseudo-molecular ion for the compounds.

High resolution accurate mass measurements (FABMS) were obtained using a VG Autospec Q mass spectrometer (accelerating voltage 8 kV; resolution 6000) and employing voltage scanning with CsI as the reference.

NMR spectroscopy

NMR Spectra were recorded on a Bruker AMX400 spectrometer. This instrument operates at 400.13 MHz for ^1H and 100.62 MHz for ^{13}C. All 2D experiments were recorded with the sample non-spinning. NMR data processing was carried out on a Bruker ASPECTstation 1 off-line processing facility with standard UXNMR software (version 940801).

All the measurements were carried out in deuteriochloroform solution at room temperature for (4-HMP)$_5$-eno-DMαCD. This was the only commonly available solvent that offered any real solubility for this compound. The same sample was used for all the NMR measurements and 90 mg of the compound were contained in 0.7 cm^3 of solvent. The solvent volume was kept constant to maintain the concentration (0.78 mol dm^{-3}) for all the measurements. Signal broadening as a result of viscosity can be a problem with CD derivatives in this solvent and the sample was investigated at 57 °C. This temperature was judged to offer little real improvement over the room temperature situation in terms of dispersion though there was some slight temperature dependence of the chemical shifts of the resonances. Room temperature was measured to be 22 °C in the probe by a Comark thermocouple placed in an NMR tube containing chloroform, and this temperature was maintained for all investigations on this sample.

The situation was more complex for (4-BOP)$_5$-eno-DMαCD because under the same conditions as those described above when dissolved in deuteriochloroform, the six anomeric protons show considerable overlap. Fortuitously, this compound was more soluble in other common solvents and in hexadeuterio-

benzene at room temperature, the anomeric protons became well-resolved. Accordingly, this solvent was used for all measurements on this compound and 20 mg were used in 0.7 cm^3 of solvent. This concentration (0.02 mol dm^{-3}) was maintained for all experiments together with an accurate temperature of 22 °C.

HOHAHA spectra were performed using the MLEV-17 sequence for isotropic mixing,[26] and in phase-sensitive mode using time proportional phase incrementation (TPPI). A 10.4 kHz spin-lock field was used and 1000 increments of 2K data points were acquired. For (4-HMP)$_5$-eno-DMαCD, a spectral width of 6.65 ppm was observed with 16 transients per increment and for (4-BOP)$_5$-eno-DMαCD, a spectral width of 5.04 ppm with 48 transients per increment was examined. The data were processed with a sine-bell window function (shifted by $\pi/2$) prior to Fourier transformation and automatic baseline correction in both domains was applied afterwards. The data in the figures is displayed with the HOHAHA cross-peaks in-phase with the diagonal and these were made to be negative and appear black. The experiment was performed twice using mixing times of 100 ms and 150 ms.

NOESY spectra[27] were recorded using similar spectral widths and digitisations to those described above for the HOHAHA experiment. A range of mixing times covering 100–400 ms was explored. An unshifted sine-bell window function was used in the processing of the data. As described in the discussion, nOe cross peaks were not observed under these conditions.

1D nOe difference spectra[28] were obtained by irradiating the peak of interest for 5 s. The multiplet was digitised and each point was irradiated for 5 ms in a cycle that was repeated one thousand times. This procedure resulted in about 90% saturation of the multiplet with suitable adjustment of the attenuation. As described in the discussion, nOe cross peaks were not observed under these conditions.

The ROESY spectra[29] were obtained using TPPI and 1000 increments of 2K data points were acquired. For (4-HMP)$_5$-eno-DMαCD, 16 transients per increment were employed together with a spectral width of 4.9 ppm. For (4-BOP)$_5$-eno-DMαCD, 40 transients per increment were used with a spectral width of 5.04 ppm. A CW spin-lock field of 2 kHz was used—significantly lower than that employed in the HOHAHA experiment to try to minimise the HOHAHA cross-peaks. To further reduce these cross-peaks, the transmitter was offset to the low-field end of the spectrum.[30] A spin-lock mixing time of 500 ms was used. The data were processed with a sine-bell window shifted by $\pi/2$ in both domains prior to Fourier transformation and automatic baseline correction was employed in both domains afterwards. The data were phased so that the HOHAHA cross-peaks were in-phase with the diagonal. These cross-peaks were made to be negative (and appear black) in the data sets displayed in the paper. The rOe cross-peaks then appear positive and are plotted red in the figures.

For coupling constant determination, a double quantum filtered (DQF) COSY experiment was performed in phase-sensitive mode using TPPI.[31] 2000 increments of 2K data points were acquired with 32 transients per increment. The data were processed with a sine-bell window shifted by $\pi/2$ in both domains prior to Fourier transformation and automatic baseline correction was employed in both domains afterwards. The data was zero-filled to 4K in both domains for the processing. For (4-HMP)$_5$-eno-DMαCD, a spectral width of 4.9 ppm was examined and for (4-BOP)$_5$-eno-DMαCD, 5.6 ppm was employed.

^{13}C NMR spectra were acquired with proton decoupling *via* the *J*-modulation (JMOD) pulse sequence[32] using a $^1J_{CH}$ coupling constant of 140 Hz.

C–H correlation spectroscopy was performed with H–H decoupling in F1 using a BIRD pulse.[33] For the (4-HMP)$_5$-eno-DMαCD experiment, the value used for $^1J_{CH}$ was 160 Hz. In the carbon domain (*F*2), a spectral width of 151 ppm was used and this domain was digitised into 2K data points. In the proton domain (*F*1), a spectral width of 6.3 ppm was used and 256 increments were employed. In *F*1, an unshifted sine-bell window function was used and in *F*2, an exponential multiplication function was employed (line-broadening factor = 15 Hz) before Fourier transformation. The data was zero-filled in *F*1 to 1K data points. The experiment was performed twice; once with 304 scans per increment and finally with 880 scans per increment with a halving of digital resolution in *F*1 in order to keep experiment time within acceptable limits.

Similar parameters were used for the (4-BOP)$_5$-eno-DMαCD experiment.

Acknowledgements

We thank Dr Sue Boyd for advice and discussion regarding the interpretation of NMR data. We thank A. H. Marks Ltd. and the SERC for financial support.

References

1 J. Szejtli, *Cyclodextrins and their Inclusion Complexes*, Akademiai Kiado, Budapest, 1982; J. Szejtli, in *Inclusion Compounds*, eds. J. L. Atwood, J. E. D. Davies and D. D. MacNicol, Academic Press, London, 1984, vol. 3, 331; M. L. Bender and M. Koniyama, *Cyclodextrin Chemistry*, Springer Verlag, Berlin, 1978.
2 W. Saenger, *Angew. Chem., Int. Ed. Engl.*, 1980, **19**, 344.
3 R. Breslow and P. Campbell, *Bioorg. Chem.*, 1971, **1**, 140.
4 M. Komiyama and H. Hirai, *Makromol. Chem., Rapid Commun.*, 1981, **2**, 715.
5 For a review of chemically modified cyclodextrins, see A. P. Croft and R. A. Bartsch, *Tetrahedron*, 1983, **39**, 2190.
6 P. Fugedi, *Carbohydrate Res.*, 1989, **192**, 365.
7 H. B. Mereyala and S. Guntha, *J. Chem. Soc., Perkin Trans. 1*, 1993, 811; K. Sato, S. Sakuma, Y. Nakamura, J. Yoshimura and H. Hashimoto, *Chem. Lett.*, 1991, 17.
8 C. M. Spencer, J. F. Stoddart and R. Zarzycki, *J. Chem. Soc., Perkin Trans. 2*, 1987, 1323; P. S. Bates, D. Parker and A. F. Patti, *J. Chem. Soc., Perkin Trans. 2*, 1994, 657; L. Jullien, J. Canceill, L. Lacombe and J.-M. Lehn, *J. Chem. Soc., Perkin Trans. 2*, 1994, 989.
9 I. Tabushi, T. Nabeshima, K. Fujita, A. Matsunaga and T. Imoto, *J. Org. Chem.*, 1985, **50**, 2638.
10 A. Bax and D. G. Davis, *J. Magn. Reson.*, 1985, **65**, 355.
11 G. Eich, G. Bodenhausen and R. R. Ernst, *J. Magn. Reson.*, 1982, **104**, 3731.
12 L. Braunschweiller and R. R. Ernst, *J. Magn. Reson.*, 1983, **53**, 521.
13 S. R. Hartmann and E. L. Hahn, *Phys. Rev.*, 1962, **128**, 2042.
14 D. P. Weitekamp, A. Bieecki, D. Zax, K. Zilm and A. Pines, *Phys. Rev. Lett.*, 1983, **50**, 1807.
15 A. Bax and D. G. Davis, *J. Magn. Reson.*, 1985, **63**, 207.
16 J. S. Waugh, *J. Magn. Reson.*, 1986, **68**, 189.
17 G. E. Martin and A. S. Zektzer, *Two-Dimensional NMR Methods for Establishing Molecular Connectivity*, VCH, Germany, 1988, p. 303.
18 P. L. Weber, L. C. Sieker, T. S. Anantha Samy, B. R. Reid and G. P. Drobny, *J. Am. Chem. Soc.*, 1987, **109**, 5842.
19 E. Breitmaier and W. Voeller, *Carbon-13 NMR Spectroscopy*, 3rd edn., VCH, Germany, 1989, p. 261.
20 An earlier NMR structural assignment on an unsymmetrical β-cyclodextrin also failed to show C6/H6 correlations in the 2D experiment. See, ref. 8.
21 M. Barfield, R. J. Spear and S. Sternhell, *Chem. Rev.*, 1976, **76**, 593.
22 Macromodel 4.0, Columbia University, 1993; see F. Mohamadi, N. G. J. Richards, W. C. Guida, R. Liskamp, M. Lipton, C. Caufield, G. Chang, T. Hendrickson and W. C. Still, *Comput. Chem.*, 1990, **11**, 440; MM3 Force Field, N. L. Allinger, Y. H. Yuh and J. H. Lii, *J. Am. Chem. Soc.*, 1989, **111**, 8551.
23 W. C. Still, A. Tempczyk, R. C. Hawley and T. Hendrickson, *J. Am. Chem. Soc.*, 1990, **112**, 6127.
24 B. Klar, B. Hingerty and W. Saenger, *Acta Crystallogr., Sect. B*, 1980, **36**, 1154.

25 Quanta 4.0, Molecular Simulation Inc. Burlington, MA, 1994. Portions of Quanta 4.0 are copyright University of York.
26 A. Bax and D. G. Davis, *J. Magn. Reson.*, 1985, **65**, 355.
27 G. Bodenhausen, H. Kogler and R. R. Ernst, *J. Magn. Reson.*, 1984, **58**, 370.
28 D. Neuhaus, *J. Magn. Reson.*, 1983, **53**, 109; M. Kinns and J. K. M. Sanders, *J. Magn. Reson.*, 1984, **56**, 518.
29 A. Bax and D. G. Davis, *J. Magn. Reson.*, 1985, **63**, 207.
30 G. Griesinger and R. R. Ernst, *J. Magn. Reson.*, 1987, **75**, 261.
31 A. E. Derome and M. Williamson, *J. Magn. Reson.*, 1990, **88**, 177.
32 C. Le Cocq and J.-Y. Lallemand, *J. Chem. Soc., Chem. Commun.*, 1981, 150.
33 A. Bax, *J. Magn. Reson.*, 1983, **53**, 517; V. Rutar, *J. Magn. Reson.*, 1984, **58**, 306; J. A. Wild and P. H. Bolton, *J. Magn. Reson.*, 1984, **59**, 343.
34 W. Saenger, *J. Am. Chem. Soc.*, 1977, **99**, 1735.
35 J. R. Johnson, N. Shankland and I. H. Sadler, *Tetrahedron*, 1985, **41**, 3147.

Paper 4/07835G
Received 23*rd December* 1994
Accepted 15*th March* 1995